NANO LETTERS

pubs.acs.org/NanoLett Letter

Universal Barcoding Predicts *In Vivo* ApoE-Independent Lipid Nanoparticle Delivery

Alejandro J. Da Silva Sanchez, Curtis Dobrowolski, Ana Cristian, Elisa Schrader Echeverri, Kun Zhao, Marine Z. C. Hatit, David Loughrey, Kalina Paunovska,* and James E. Dahlman*

Cite This: https://doi.org/10.1021/acs.nanolett.2c01133 Read Online

ACCESS | Metrics & More | Article Recommendations | Supporting Information

ABSTRACT: To predict whether preclinical lipid nanoparticle (LNP) delivery will translate in humans, it is necessary to understand whether the mechanism used by LNPs to enter cells is conserved across species. In mice, non-human primates, and humans, LNPs deliver RNA to hepatocytes by adsorbing apolipoprotein E (ApoE), which binds low-density lipoprotein receptor (LDLR). A growing number of LNPs can deliver RNA to nonhepatocytes, suggesting that ApoE- and LDLR-independent interactions could affect LNP tropism. To evaluate this hypothesis, we developed a universal DNA barcoding system that quantifies how chemically distinct LNPs deliver small interfering RNA in any mouse model, including genetic knockouts. We quantified how 98 different LNPs targeted 11 cell types in wildtype, LDLR$^{-/-}$, very low-density lipoprotein receptor, and ApoE$^{-/-}$ mice, studying how these genes, which traffic endogenous lipids, affected LNP delivery. These data identified a novel, stereopure LNP that targets Kupffer cells, endothelial cells, and hepatocytes in an ApoE-independent manner. These results suggest that non-ApoE interactions can affect the tropism of LNP-RNA drugs.

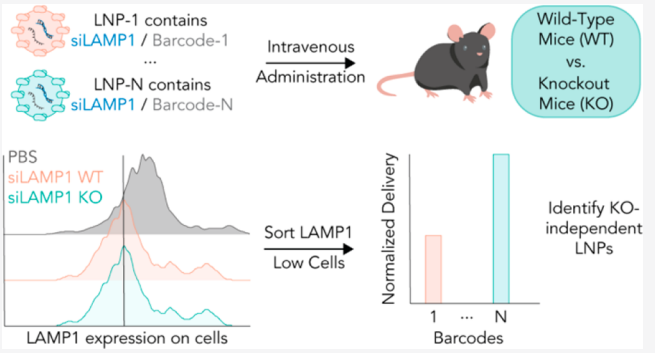

KEYWORDS: *DNA barcode, LNP, lipid nanoparticle, siRNA, knockout*

INTRODUCTION

In 2018, the Food and Drug Administration (FDA) approved patisiran, a lipid nanoparticle (LNP) that delivers small interfering RNA (siRNA) targeting transthyretin to hepatocytes.[1] More recently, LNPs carrying mRNA encoding Cas9 and single-guide RNA (sgRNA) led to hepatocyte gene editing in nonhuman primates (NHPs)[2,3] and humans.[4] These LNPs enter hepatocytes by adsorbing serum apolipoprotein E (ApoE), which leads to subsequent low-density lipoprotein receptor (LDLR)-mediated uptake.[5] In a second example, the FDA and European Medicines Agency approved[6−8] siRNA conjugated to N-acetylgalactosamine (GalNAc), which enters hepatocytes by binding the asialoglycoprotein receptor (ASGPR).[9] Both ApoE/LDLR and GalNAc/ASGPR are conserved in mice, rats, NHPs, and humans, underscoring the value of understanding mechanisms that influence *in vivo* delivery.

After surveying the literature, we found ApoE-independent LNP delivery to be rarely reported *in vivo* with two exceptions. In the first, an ionizable LNP based on Dlin-KC2-DMA was found to be ApoE-dependent, whereas LNPs containing the cationic lipid 98N$_{12}$ were ApoE-independent.[10] In the second, LNPs formulated with the ionizable lipid DLin-MC3-DMA were shown to deliver mRNA to the eye in ApoE$^{-/-}$ mice after subretinal injection.[11] However, three key lines of evidence suggest that ApoE-independent LNP trafficking may be more common than currently thought. First, endogenous lipids are trafficked to many nonhepatocyte cell types. Second, lipid trafficking involves many genes, not just ApoE.[12,13] Third, an increasing number of LNPs administered intravenously have delivered RNA to nonhepatocytes without the use of active targeting ligands such as antibodies or aptamers,[14−18] suggesting that LNPs may interact with serum components that leverage different receptors to enter cells.[19]

RESULTS

Identifying an LNP with ApoE-independent *in vivo* tropism has been difficult in part because rigorous studies are difficult to execute. Specifically, an ideal "biology of delivery" study would be characterized by four key traits (Figure 1A). First, it would be performed with many nanoparticles to ensure the results are robust across chemical structures. Second, the study would evaluate how several genes on the same pathway influence

Received: March 21, 2022
Revised: May 13, 2022

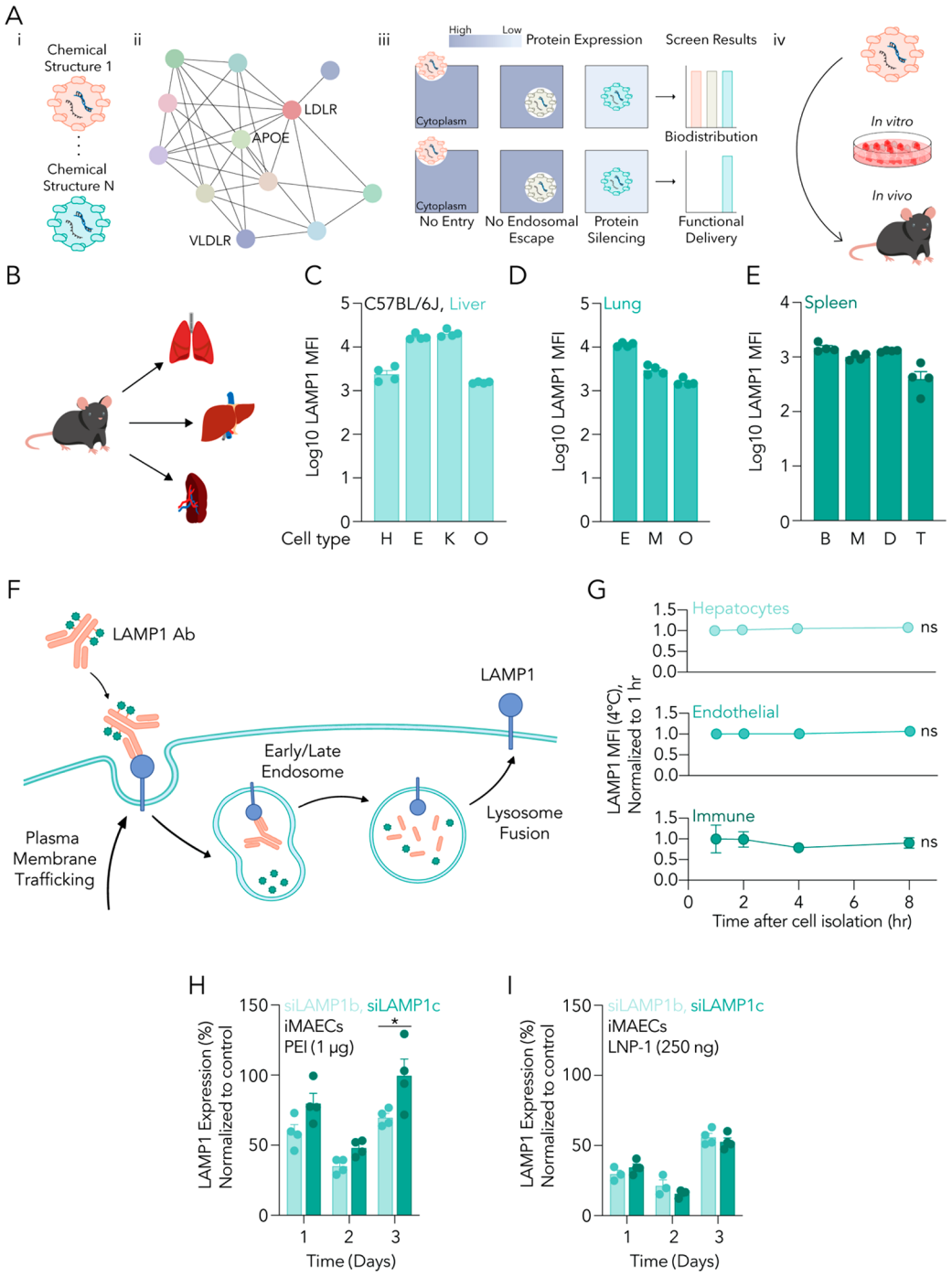

Figure 1. LAMP1 meets the criteria for an siRNA-based screening system. (A) Four criteria (i–iv) exist for an ideal siRNA screening system. (B) LAMP1 protein is ubiquitously expressed across many tissues. LAMP1 surface expression levels are stable across multiple mice for cell types in (C) the liver, (D) the lung, and (E) the spleen. (F) LAMP1 cell surface expression must be stable over time to qualify as a candidate protein. (G) LAMP1 cell surface expression is stable over 8 h in liver hepatocytes, endothelial cells, and immune cells *in vivo*. Sequences siLAMP1b and siLAMP1c led to potent silencing *in vitro* when delivered using (H) PEI and (I) LNP-1. For Figure 1G, statistical analyses were conducted using linear regression and testing for the significance of the slope parameter being different from zero. For Figure 1H, I, statistical analyses were conducted using a two-factor ANOVA between LAMP1 expression after siLAMP1b or siLAMP1c administration at each time point with Šidák's multiple comparison test at every time point. ns ($p > 0.05$, not shown), * ($p < 0.05$).

delivery. Third, given that many of these genes are likely involved in endocytosis[20] and that endosomal escape can be inefficient,[21] the study would quantify how the siRNA is functionally delivered (i.e., siRNA-mediated target protein reduction) rather than measuring nanoparticle biodistribution (i.e., only where the nanoparticle went). Fourth, the assays would be performed directly *in vivo*, since delivery in cell culture can be a poor predictor of nanoparticle delivery *in vivo*.[22] However, a study with these four traits would normally require several hundred genetically engineered animals, which is expensive and unethical. To enable these studies, here we designed, characterized, and validated a system that quantifies

https://doi.org/10.1021/acs.nanolett.2c01133
Nano Lett. XXXX, XXX, XXX−XXX

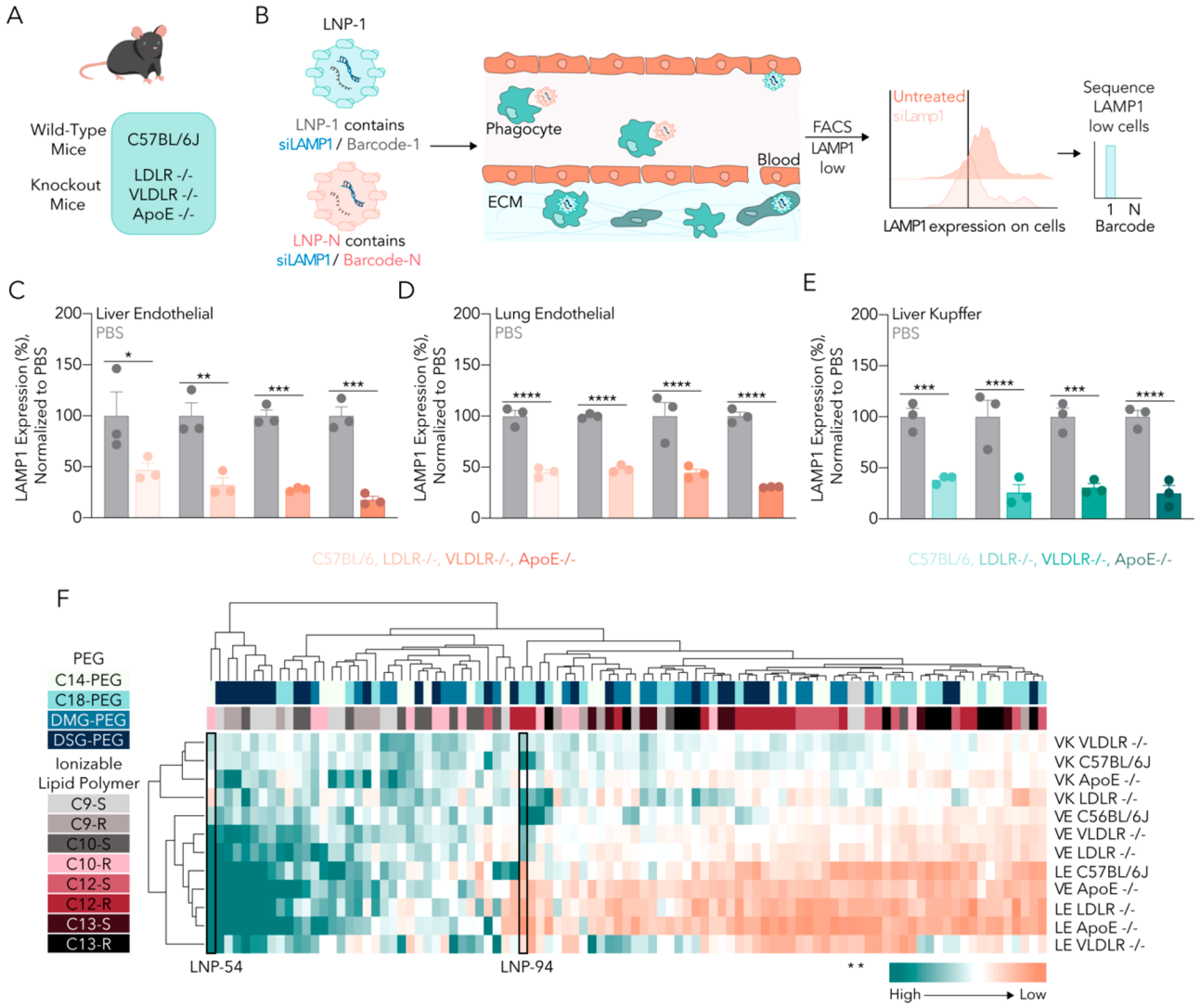

Figure 2. Lipid nanoparticles can be screened in knockout mice using siRNA against LAMP1. (A) The novel siLAMP1 system can be applied to identify LNPs that are knockout-independent by administering LNPs to wildtype and knockout mice. (B) LNPs are formulated to carry siLAMP1 and a DNA barcode; cells with lower LAMP1 expression are sorted and sequenced to identify winning LNPs. We observed statistically significant LAMP1 protein silencing in every mouse strain in (C) liver endothelial cells, (D) lung endothelial cells, and (E) liver Kupffer cells. (F) Heatmap showing the normalized barcode delivery of each LNP for every cell type, tissue, and mouse strain sequenced. Naked barcodes are represented by "*" and delivery profiles of LNP-54 and LNP-94 are highlighted. Statistical analyses were conducted using a two-factor ANOVA between PBS control and mice receiving siLAMP1 with Šidák's multiple comparison test at every mouse model. * ($p < 0.05$), ** ($p < 0.01$), *** ($p < 0.001$), **** ($p < 0.0001$). VK, liver Kupffer cells; VE, liver endothelial cells; LE, lung endothelial cells.

how dozens of different LNPs functionally deliver siRNA to any combination of cell types, in any desired mouse model, including genetic knockouts. We then used the system to evaluate how a systematic panel of 98 LNPs delivered siRNA in wildtype C57BL/6J (WT), ApoE$^{-/-}$, LDLR$^{-/-}$, and very low-density lipoprotein receptor (VLDLR$^{-/-}$) knockout mice. We chose ApoE$^{-/-}$ and LDLR$^{-/-}$ for their role in endocytosis of the clinically approved nanoparticle Onpattro.[10] We also chose VLDLR$^{-/-}$ for two reasons: (i) naturally occurring VLDL has a similar size to LNPs,[23] and (ii) novel ionizable lipids might not depend on ApoE and LDLR for entry. Using this system, we identified two LNPs, named LNP-54 and LNP-94, which deliver siRNA to liver Kupffer cells, lung endothelial cells and, in the case of LNP-54, liver endothelial cells, in an ApoE-independent manner. More broadly, these results suggest that universal DNA barcoding can identify how specific genes do or do not influence LNP delivery to target cells.

We reasoned that this siRNA barcoding system would require a gene that was expressed ubiquitously across cell types. Furthermore, the gene would encode a protein with cell surface expression, thereby enabling measurements of siRNA-mediated silencing with cellular resolution using flow cytometry, rather than tissue-level readouts. Finally, silencing an ideal target gene would not lead to dysregulated growth or immune clearance, as both of these would underreport delivery. To identify a gene with these properties, we surveyed the Human Protein Atlas[24] and selected the lysosomal-associated membrane protein 1 (LAMP1) for further investigation. LAMP1 is a component of lysosomal membranes, where it maintains endocytic compartments and participates in autophagy.[25] Importantly, LAMP1 silencing does not affect animal physiology: *Lamp1* knockouts are viable

https://doi.org/10.1021/acs.nanolett.2c01133
Nano Lett. XXXX, XXX, XXX−XXX

and fertile; they possess unaffected lysosomal properties; and *Lamp1* deficiency is counterbalanced by *Lamp2* upregulation.[25,26]

Since LAMP1 has been detected on the plasma membrane,[27−29] we hypothesized that we could quantify LAMP1 protein, and thus siRNA-mediated silencing, after LNP delivery of siLAMP1 using flow cytometry. We therefore analyzed LAMP1 mean fluorescence intensity (MFI) on 11 cell types isolated from the liver, lung, and spleen (Figure 1B). We sacrificed C57BL/6J mice, digested tissues into single-cell suspensions, and found that LAMP1 was expressed on all tested cell types (Figure 1C−E). Specifically, we detected consistent LAMP1 MFI on liver hepatocytes (H), lung and liver endothelial cells (E), liver Kupffer cells (K), lung and spleen macrophages (M), spleen B cells (B), T cells (T), dendritic cells (D), and other immune cells in liver and lung (O). To evaluate whether *Lamp1* expression varied with the genetic background, we repeated the experiment with Balb/c (Figure S1A−C) and 129 S1 mice (Figure S1D−F) and found LAMP1 on all tested cells. Since plasma membrane LAMP1 can be internalized and shuttled to lysosomes for degradation,[29] we reasoned that LAMP1 signal could decrease over time after it was bound by an antibody, thereby overreporting siRNA-mediated LAMP1 silencing in samples analyzed later in a long experiment, compared to samples analyzed earlier (Figure 1F). We therefore isolated cells from C57BL/6J mice, stained them with anti-LAMP1 antibody, and stored them at 4 °C (Figure 1G) or on ice for 8 h (Figure S1G); LAMP1 MFI did not change significantly.

We then evaluated four siRNAs targeting *Lamp1* mRNA, which we named siLAMP1a−siLAMP1d (Figure S1H). All four sequences were chemically modified for *in vivo* studies by adding 2′-O-methyl and phosphorothioate bonds.[30] We compared the potency of siLAMP1a-d *in vitro* using two delivery systems: poly(ethylenimine) (PEI) (Figure 1H, Figure S1I) or a validated lung-targeting LNP,[17] which we named LNP-1 (Figure 1I, Figure S1J,K). After finding that siLAMP1b and siLAMP1c were the most potent *in vitro* (Figure 1H,I), we formulated LNP-1 with siLAMP1b or siLAMP1c and intravenously injected it into WT mice at a dose of 1.5 mg/kg (Figure S1L−O). Three days later, we observed 55% silencing in hepatocytes (Figure S1M), 51% silencing in liver endothelial cells (Figure S1N), and 32% silencing in lung endothelial cells (Figure S1O) in mice treated with siLAMP1b, compared to mice treated with PBS. We did not observe LAMP1 silencing in mice injected with a control siRNA targeting luciferase (siLuc). Mice treated with siLAMP1b or siLAMP1c did not lose weight compared to mice treated with 1X PBS or mice treated with LNP-1 containing siLuc (Figure S1L). We selected siLAMP1b for subsequent studies and renamed it siLAMP1 for simplicity.

We then used this siLAMP1 to perform a high-throughput *in vivo* screen of novel, stereopure LNPs in WT, ApoE$^{-/-}$, LDLR$^{-/-}$, and VLDLR$^{-/-}$ mice with the goal of identifying LNPs that targeted hepatic and nonhepatic cells via ApoE-independent mechanisms (Figure 2A). We used stereopure compounds to avoid batch-to-batch variability issues that arise due to the chiral centers of an ionizable lipid. We first synthesized the stereopure lipids by reacting low molecular weight poly(ethylenimine) (PEI$_{600}$) to chiral epoxides using an epoxide ring-opening reaction (Figure S2A,B) and characterized them using ^{1}H NMR (Figure S2C−J). Using these stereopure lipids, we created a systematic panel of 128 chemically distinct DNA-barcoded LNPs via microfluidics.[31] Specifically, LNP-1 was formulated to carry siLAMP1 and DNA barcode 1, whereas LNP-N was formulated to carry siLAMP1 and DNA barcode N (Figure 2B, Figure S3A). By using DNA barcodes that were rationally designed to be highly sensitive readouts of *in vivo* delivery (Figure S3B),[32] we were able to use a 10:1 mass ratio of siRNA:DNA barcode. We focused on LNPs with three constituents: an ionizable lipid polymer, a PEG-lipid, and cholesterol, a composition that has potently delivered siRNA to endothelial cells on multiple tissues.[15] These components are similar to those used in clinical LNPs made by Alnylam,[1] Moderna,[33] and Acuitas/BioNTech/Pfizer.[34] Specifically, we diversified the structure of the ionizable lipid with the eight novel, stereopure 7C1-based[15] lipid-polymers that we synthesized (Figure S2A,B, Figure S3C). Since previous studies have shown that PEG-lipid content and structure influence LNP pharmacokinetics and delivery,[35] we diversified the library by using four PEG-lipids (Figure S3D). Finally, to ensure our results were not specific to one molar ratio, we formulated the LNPs using four different molar ratios (Figure S3E). Thus, each of the eight stereopure lipids was formulated 16 different ways (four PEG-lipids and four molar ratios).

After formulating the 128 LNPs, we measured the hydrodynamic diameter of each formulation with dynamic light scattering (DLS), then pooled the 98 LNPs with monodisperse DLS spectra and diameters between 30 and 150 nm; the remaining 30 LNPs were discarded. As a control, we measured the diameter of the pool and found it to be within the range of the individual LNPs in the pool, suggesting that the LNPs were stable after mixing (Figure S3F). As a second control, we included two unencapsulated DNA barcodes. Since DNA barcodes do not readily enter cells without a delivery vehicle, the unencapsulated DNA should be delivered less efficiently than barcodes within LNPs. We then analyzed whether LNP chemistry affected formulation success (Figure S3G), hydrodynamic diameter (Figure S3H), and the polydispersity index (Figure S3I) of the LNPs. We defined formulation success as LNPs having monodisperse diameter distributions with diameters between 30 and 150 nm (Figure S3J). Even though we did not find any trends that dictated whether individual LNPs would formulate, these data led us to conclude that stereopure lipids can be used to formulate stable LNPs.

We then intravenously injected the LNPs at a total nucleic acid dose of 1.5 mg/kg (i.e., 0.015 mg/kg for each of the 98 LNPs, on average). Seventy-two hours later, we isolated the lung, liver, and spleen and quantified LAMP1 MFI. Compared to control mice treated with 1X PBS, we observed a 53%, 55%, and 61% reduction in LAMP1 in liver endothelial cells (Figure 2C), lung endothelial cells (Figure 2D), and liver Kupffer cells (Figure 2E) in WT mice, respectively. We observed less LAMP1 silencing in eight other cell types (Figure S4), including hepatocytes. We then evaluated the effect of LDLR, VLDLR, and ApoE absence on delivery by measuring LAMP1 silencing in knockout mice. Contrasting the behavior of ApoE-dependent LNPs, which deliver less drug in ApoE$^{-/-}$ mice than in WT mice,[10] we found that LAMP1 silencing, barring some small differences, was similar in all three knockout mice as well as WT mice (Figure 2C−E, Figure S4A−C). Notably, we found differences in hepatocyte LAMP1 silencing to be negligible across mouse strains (Figure S4A). These data provide one line of evidence that the LNPs, which exhibited

https://doi.org/10.1021/acs.nanolett.2c01133
Nano Lett. XXXX, XXX, XXX−XXX

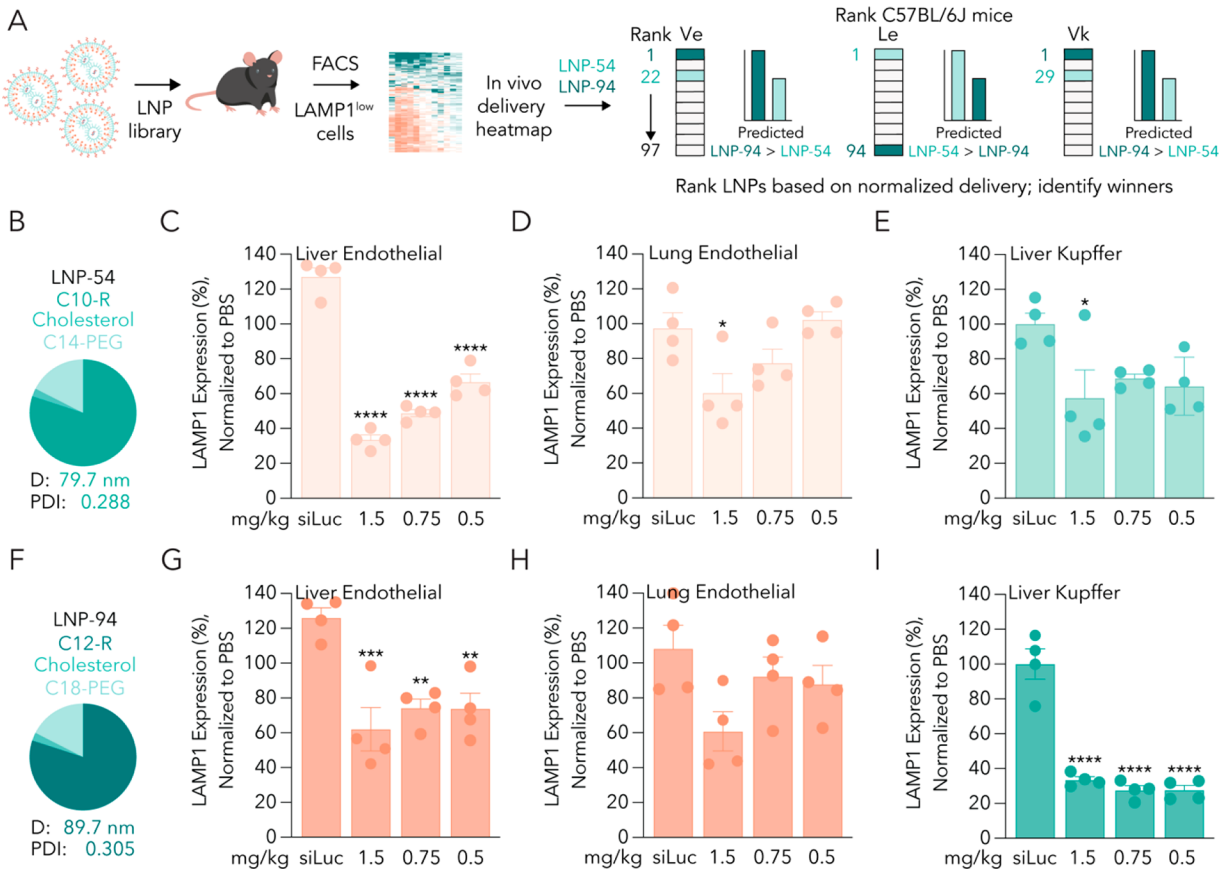

Figure 3. LNP screening allows us to find LNPs with specific tissue and cell tropisms. (A) Two LNPs identified had differential performance in the lung and liver in C57BL/6J mice. The performance of (B) LNP-54 was evaluated in (C) liver endothelial, (D) lung endothelial, and (E) liver Kupffer cells. Similarly, the performance of (F) LNP-94 was evaluated in (G) liver endothelial, (H) lung endothelial, and (I) liver Kupffer cells. Statistical analyses were conducted using a one-way ANOVA with Tukey's multiple comparison test. Statistical differences shown compare LAMP1 protein expression of mice receiving siLAMP1 against mice receiving siLuc. ns ($p > 0.05$, not shown), * ($p < 0.05$), ** ($p < 0.01$), *** ($p < 0.001$), **** ($p < 0.0001$). VK, liver Kupffer cells; VE, liver endothelial cells; LE, lung endothelial cells.

preferential tropism to nonhepatocytes, did not require LDLR, VLDLR, or ApoE to deliver siRNA to target cells.

One advantage of DNA barcoding studies is the ability to measure how many different LNPs behave *in vivo*. We therefore used next-generation sequencing (NGS) to quantify the normalized delivery of all 98 barcodes in the cell types where we observed the most robust silencing: lung endothelial cells, liver endothelial cells, and liver Kupffer cells (Figure 2C–E). Normalized delivery is used to quantify barcode delivery[16,32] and is detailed in Figure S5. The unencapsulated DNA barcodes, which serve as negative sequencing controls, were among the lowest in all cell types sequenced across all animal models (Figure S6A), validating our normalized delivery data. We also plotted normalized delivery as a function of LNP hydrodynamic diameter and found no relationship between LNP diameter and delivery within the size range tested (Figure S6B) and no relationship between LNP PDI an delivery (Figure S6C); this is consistent with previous studies.[14,22]

After evaluating the sequencing controls, we performed unbiased clustering[36,37] on the normalized delivery of all the LNPs in all cell types and animal models sequenced (Figure 2F, Figure S6D). The barcode sequencing data identified two LNPs with different tropisms. The first LNP, which we named LNP-54, had the highest normalized delivery in WT lung endothelial cells (Figure 3A). The second LNP, which we named LNP-94, had higher normalized delivery in WT liver endothelial and liver Kupffer. We noticed both LNPs contained the molar ratio 80:2.5:17.5 of ionizable lipid : cholesterol : PEG lipid. This was a ratio we found present among other top performing LNPs. To confirm these observations from the sequencing data, we formulated LNP-54 (Figure 3B) with siLAMP1 and administered the LNPs at doses of 1.5, 0.75, or 0.5 mg/kg to WT mice. As a control, we also injected siLuc at a dose of 1.5 mg/kg. We then evaluated LAMP1 protein expression in liver endothelial cells, lung endothelial cells, and liver Kupffer cells (Figure 3C–E). Compared to PBS-treated mice, we observed 66% LAMP1 protein silencing in liver endothelial cells, 42% LAMP1 silencing in Kupffer cells, and 40% LAMP1 silencing in lung endothelial cells at the highest dose tested. We repeated the experiment, this time formulating LNP-94 (Figure 3F) with siLuc or siLAMP1. At the highest dose tested, LNP-94 reduced LAMP1 expression in liver and lung endothelial cells by 38% and 39%, respectively (Figure 3G,H) and silenced LAMP1 protein in Kupffer cells by 70% at doses as low as 0.5 mg/kg (Figure 3I). As initially predicted by the screen, LNP-54 performed better in lung endothelial cells compared to LNP-94 and LNP-94 performed better in liver Kupffer cells than LNP-54 (Figure 3A). We did not observe a better performance of LNP-94 in liver endothelial cells compared to LNP-54 as the sequencing data originally suggested. However, the screen

https://doi.org/10.1021/acs.nanolett.2c01133
Nano Lett. XXXX, XXX, XXX−XXX

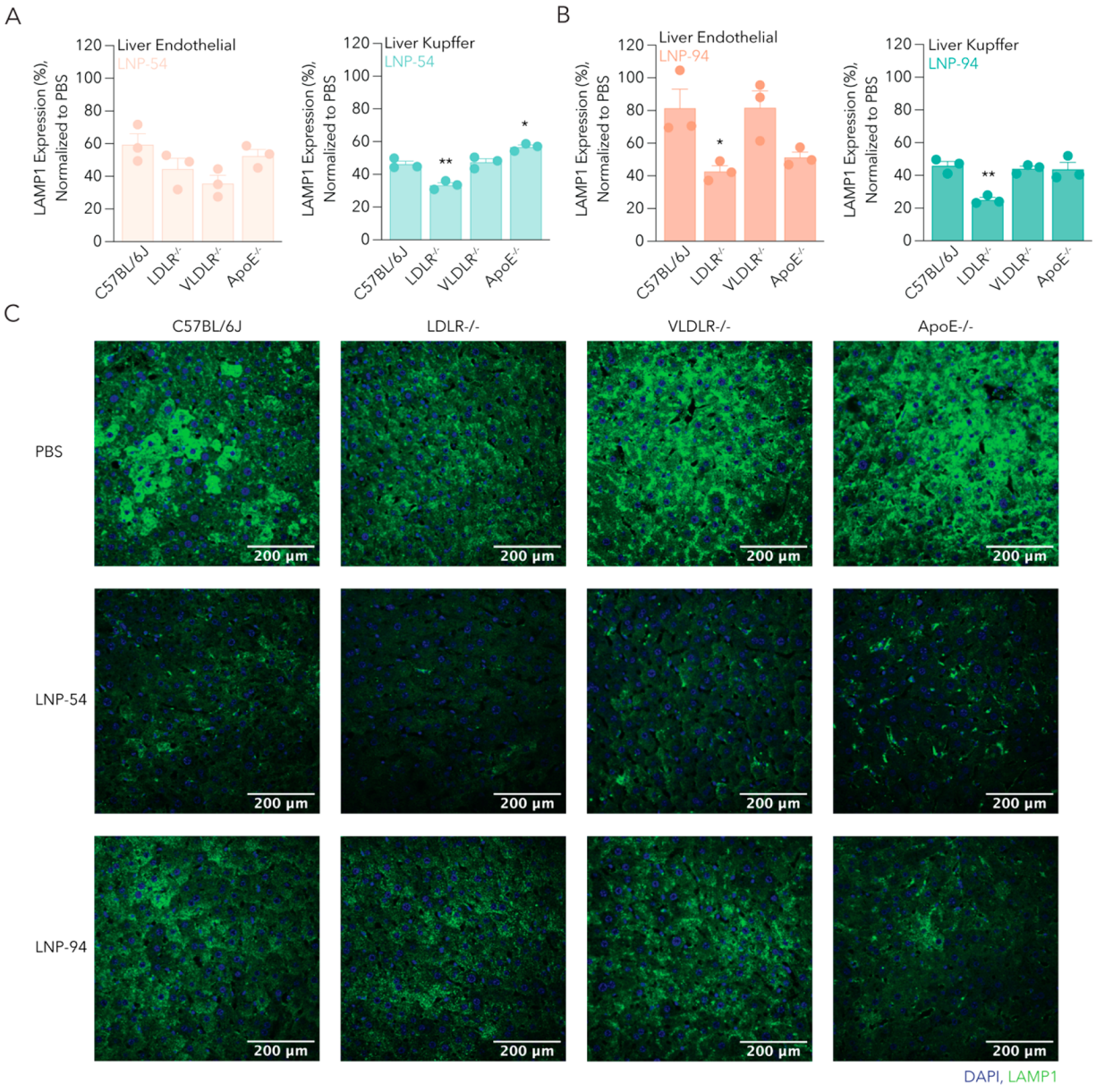

Figure 4. LNP-54 and LNP-94 are ApoE-independent. (A) The performance of LNP-54 in liver endothelial and Kupffer cells was evaluated across all mouse models. Similarly, (B) the performance of LNP-94 in liver endothelial and Kupffer cells was evaluated in all mouse models. (C) Qualitative comparison of AF488 pixel intensity of liver sections of mice treated with siLAMP1 or PBS across all mouse models. Statistical analyses were conducted using a one-way ANOVA with Tukey's multiple comparison test. Statistical differences shown compare LAMP1 protein expression of genetic knockout mice against C57BL/6J control. ns ($p > 0.05$, not shown), * ($p < 0.05$), ** ($p < 0.01$).

predicted LNP-54 to be better than LNP-94 in liver endothelial cells across all knockout mice, which made us believe that some sequencing bias might have occurred during NGS for LNP-54 in C57BL/6J liver endothelial cells (Figure S7). We also cannot discard the possibility that more LNP-94 was endocytosed in C57BL/6J mice without its payload being necessarily released into the cytoplasm (Figure 1A). Finally, compared to mice treated with PBS, we observed no changes in weight or liver histology after mice were treated with LNP-54 or LNP-94 (Figure S8A,B).

After confirming the activity of LNP-54 and LNP-94 in WT mice, we evaluated how the LNPs delivered siLAMP1 in knockout mice. In previous studies, LNPs that were ApoE-dependent silenced genes far less efficiently in ApoE$^{-/-}$ mice compared to WT mice, whereas ApoE-independent LNPs silenced genes with approximately the same efficiency in both models.[10] We therefore injected LNP-54 into all three knockout models at a dose of 0.75 mg/kg and compared LAMP1 silencing to WT mice treated with the same dose. We did not observe consistently worse delivery in ApoE$^{-/-}$ mice (Figure 4A, Figure S9A,B), compared to WT mice. We then repeated the experiment with LNP-94 and made similar observations (Figure 4B, Figure S9C,D). Interestingly, we observed better delivery in LDLR$^{-/-}$ across most cell types; it is possible that competing endocytosis mechanisms that do not depend on LDLR are more efficient for siRNA delivery and the lack of LDLR favors these mechanisms. We confirmed these flow cytometry-based readouts by quantifying tissue-level LAMP1 expression using confocal microscopy (Figure 4C, Figure S9E). While LNP-54 showed similar silencing levels to

https://doi.org/10.1021/acs.nanolett.2c01133
Nano Lett. XXXX, XXX, XXX−XXX

the flow cytometry data, LNP-94 showed an opposing performance in LDLR$^{-/-}$ and VLDLR$^{-/-}$ mice compared to the flow cytometry data set. Given that LAMP1 is highly enriched in late endosomes and lysosomes, we anticipate that lead LNPs must confirm intracellular and surface-level silencing to ensure consistent results. Finally, as a positive control we injected the LNP used to deliver patisiran with siLAMP1 as the payload to WT, LDLR$^{-/-}$, and ApoE$^{-/-}$ mice at a dose of 0.3 mg/kg (Figure S9F). Previous research has shown that this LNP is reliant on ApoE and LDLR to deliver siRNA, and because of this we did not think it necessary to validate dependence on VLDLR.[5] As expected, we observed significantly lower delivery in the knockout mice compared to WT mice across multiple liver cell types (Figure S9G). Taken together, these data suggest that LNP-54 and LNP-94 target cells in an ApoE-independent manner.

DISCUSSION

Both FDA-approved hepatocyte-targeting RNA delivery systems enter cells using pathways that are conserved across preclinical species and humans. Thus, to speed the development of delivery systems that target nonhepatocytes, it will be important to understand the genes that promote delivery to new cells. Here, we characterize a novel universal barcoding platform with the aim of discovering ApoE-independent LNPs for siRNA delivery. Notably, both LNP-54 and LNP-94 did not seem to require ApoE, and both LNPs tended to preferentially deliver siRNA to nonhepatocytes. Although the data are early, they support the hypothesis that non-ApoE serum interactions may be exploited to target new cell types.

This assay is distinct from an siGFP-based barcoding system we recently reported;[16] the previous siGFP system required mice that constitutively express GFP, and thus cannot easily be used to study knockout mice. Although we focused our studies on mice, it is feasible that similar approaches could be used to perform high-throughput screens in other species, including larger animals. Notably, we found that LAMP1 is expressed across several species, including rats[38] and nonhuman primates.[39] At the same time, it is important to acknowledge the limitations of this work. First, although we identified that LNP-54 and LNP-94 did not depend on ApoE, we did not identify novel genes that are required for their delivery. Further studies involving other knockout mice or RNA sequencing might be needed to identify the mechanism by which these LNPs enter cells and deliver their cargo. Second, this LAMP1 system is currently limited to mice; it is possible that the genes that affect delivery in NHPs may differ.[40] Third, we identified LNP-54 and LNP-94 by their efficiency in silencing LAMP1; studies about their pharmacokinetics, biodistribution, protein corona formed in serum, and stability over time remain to be determined. Finally, all LNPs were administered intravenously; we cannot discard the possibility that these LNPs might behave differently if injected through different routes of administration. Despite the limitations, the ability to rapidly evaluate how genes influence LNP-mediated RNA delivery in mice may be useful in understanding how we can use delivery systems to target new cell types.[41]

ASSOCIATED CONTENT

Supporting Information

The Supporting Information is available free of charge at https://pubs.acs.org/doi/10.1021/acs.nanolett.2c01133.

Experimental methods and supplementary figures (PDF)

AUTHOR INFORMATION

Corresponding Authors

Kalina Paunovska − *Wallace H. Coulter Department of Biomedical Engineering, Georgia Institute of Technology, Atlanta, Georgia 30332, United States*; Email: kpaunovska3@gatech.edu

James E. Dahlman − *Wallace H. Coulter Department of Biomedical Engineering, Georgia Institute of Technology, Atlanta, Georgia 30332, United States*; orcid.org/0000-0001-7580-436X; Email: james.dahlman@bme.gatech.edu

Authors

Alejandro J. Da Silva Sanchez − *Petit Institute for Bioengineering and Biosciences, Georgia Institute of Technology, Atlanta, Georgia 30332, United States; Department of Chemical Engineering, Georgia Institute of Technology, Atlanta, Georgia 30332, United States*

Curtis Dobrowolski − *Wallace H. Coulter Department of Biomedical Engineering, Georgia Institute of Technology, Atlanta, Georgia 30332, United States*

Ana Cristian − *Wallace H. Coulter Department of Biomedical Engineering, Georgia Institute of Technology, Atlanta, Georgia 30332, United States*

Elisa Schrader Echeverri − *Wallace H. Coulter Department of Biomedical Engineering, Georgia Institute of Technology, Atlanta, Georgia 30332, United States*

Kun Zhao − *Wallace H. Coulter Department of Biomedical Engineering, Georgia Institute of Technology, Atlanta, Georgia 30332, United States;* Present Address: Key Laboratory of Chemical Biology (Ministry of Education), School of Pharmaceutical Sciences, Shandong University, Jinan 250012, P.R. China

Marine Z. C. Hatit − *Wallace H. Coulter Department of Biomedical Engineering, Georgia Institute of Technology, Atlanta, Georgia 30332, United States*

David Loughrey − *Wallace H. Coulter Department of Biomedical Engineering, Georgia Institute of Technology, Atlanta, Georgia 30332, United States*

Complete contact information is available at: https://pubs.acs.org/10.1021/acs.nanolett.2c01133

Author Contributions

A.J.D.S., K.P., and J.E.D. designed experiments. A.J.D.S. and K.P. performed the experiments with help from the other authors. A.J.D.S. and K.P. analyzed the data. A.J.D.S., K.P., and J.E.D. wrote the paper with input from all authors.

Funding

This work was funded by DARPA (PREPARE Grant HR00111920008, awarded to J.E.D).

Notes

The authors declare the following competing financial interest(s): J.E.D. is an advisor to Google Ventures.

ACKNOWLEDGMENTS

The authors thank Karen Tiegren.

REFERENCES

(1) Adams, D.; Gonzalez-Duarte, A.; O'Riordan, W. D.; Yang, C. C.; Ueda, M.; Kristen, A. V.; Tournev, I.; Schmidt, H. H.; Coelho, T.; Berk, J. L.; Lin, K. P.; Vita, G.; Attarian, S.; Plante-Bordeneuve, V.;

Mezei, M. M.; Campistol, J. M.; Buades, J.; Brannagan, T. H., 3rd; Kim, B. J.; Oh, J.; Parman, Y.; Sekijima, Y.; Hawkins, P. N.; Solomon, S. D.; Polydefkis, M.; Dyck, P. J.; Gandhi, P. J.; Goyal, S.; Chen, J.; Strahs, A. L.; Nochur, S. V.; Sweetser, M. T.; Garg, P. P.; Vaishnaw, A. K.; Gollob, J. A.; Suhr, O. B. Patisiran, an RNAi Therapeutic, for Hereditary Transthyretin Amyloidosis. *New England journal of medicine* **2018**, *379* (1), 11−21.

(2) Musunuru, K.; Chadwick, A. C.; Mizoguchi, T.; Garcia, S. P.; DeNizio, J. E.; Reiss, C. W.; Wang, K.; Iyer, S.; Dutta, C.; Clendaniel, V.; Amaonye, M.; Beach, A.; Berth, K.; Biswas, S.; Braun, M. C.; Chen, H.-M.; Colace, T. V.; Ganey, J. D.; Gangopadhyay, S. A.; Garrity, R.; Kasiewicz, L. N.; Lavoie, J.; Madsen, J. A.; Matsumoto, Y.; Mazzola, A. M.; Nasrullah, Y. S.; Nneji, J.; Ren, H.; Sanjeev, A.; Shay, M.; Stahley, M. R.; Fan, S. H. Y.; Tam, Y. K.; Gaudelli, N. M.; Ciaramella, G.; Stolz, L. E.; Malyala, P.; Cheng, C. J.; Rajeev, K. G.; Rohde, E.; Bellinger, A. M.; Kathiresan, S. In vivo CRISPR base editing of PCSK9 durably lowers cholesterol in primates. *Nature* **2021**, *593* (7859), 429−434.

(3) Rothgangl, T.; Dennis, M. K.; Lin, P. J. C.; Oka, R.; Witzigmann, D.; Villiger, L.; Qi, W.; Hruzova, M.; Kissling, L.; Lenggenhager, D.; Borrelli, C.; Egli, S.; Frey, N.; Bakker, N.; Walker, J. A., 2nd; Kadina, A. P.; Victorov, D. V.; Pacesa, M.; Kreutzer, S.; Kontarakis, Z.; Moor, A.; Jinek, M.; Weissman, D.; Stoffel, M.; van Boxtel, R.; Holden, K.; Pardi, N.; Thony, B.; Haberle, J.; Tam, Y. K.; Semple, S. C.; Schwank, G. In vivo adenine base editing of PCSK9 in macaques reduces LDL cholesterol levels. *Nat. Biotechnol.* **2021**, *39* (8), 949−957.

(4) Gillmore, J. D.; Gane, E.; Taubel, J.; Kao, J.; Fontana, M.; Maitland, M. L.; Seitzer, J.; O'Connell, D.; Walsh, K. R.; Wood, K.; Phillips, J.; Xu, Y.; Amaral, A.; Boyd, A. P.; Cehelsky, J. E.; McKee, M. D.; Schiermeier, A.; Harari, O.; Murphy, A.; Kyratsous, C. A.; Zambrowicz, B.; Soltys, R.; Gutstein, D. E.; Leonard, J.; Sepp-Lorenzino, L.; Lebwohl, D. CRISPR-Cas9 In Vivo Gene Editing for Transthyretin Amyloidosis. *N Engl J. Med.* **2021**, *385* (6), 493−502.

(5) Akinc, A.; Maier, M. A.; Manoharan, M.; Fitzgerald, K.; Jayaraman, M.; Barros, S.; Ansell, S.; Du, X.; Hope, M. J.; Madden, T. D.; Mui, B. L.; Semple, S. C.; Tam, Y. K.; Ciufolini, M.; Witzigmann, D.; Kulkarni, J. A.; van der Meel, R.; Cullis, P. R. The Onpattro story and the clinical translation of nanomedicines containing nucleic acid-based drugs. *Nat. Nanotechnol* **2019**, *14* (12), 1084−1087.

(6) Balwani, M.; Sardh, E.; Ventura, P.; Peiró, P. A.; Rees, D. C.; Stölzel, U.; Bissell, D. M.; Bonkovsky, H. L.; Windyga, J.; Anderson, K. E.; Parker, C.; Silver, S. M.; Keel, S. B.; Wang, J. D.; Stein, P. E.; Harper, P.; Vassiliou, D.; Wang, B.; Phillips, J.; Ivanova, A.; Langendonk, J. G.; Kauppinen, R.; Minder, E.; Horie, Y.; Penz, C.; Chen, J.; Liu, S.; Ko, J. J.; Sweetser, M. T.; Garg, P.; Vaishnaw, A.; Kim, J. B.; Simon, A. R.; Gouya, L. Phase 3 Trial of RNAi Therapeutic Givosiran for Acute Intermittent Porphyria. *New England journal of medicine* **2020**, *382* (24), 2289−2301.

(7) Garrelfs, S. F.; Frishberg, Y.; Hulton, S. A.; Koren, M. J.; O'Riordan, W. D.; Cochat, P.; Deschênes, G.; Shasha-Lavsky, H.; Saland, J. M.; Van't Hoff, W. G.; Fuster, D. G.; Magen, D.; Moochhala, S. H.; Schalk, G.; Simkova, E.; Groothoff, J. W.; Sas, D. J.; Meliambro, K. A.; Lu, J.; Sweetser, M. T.; Garg, P. P.; Vaishnaw, A. K.; Gansner, J. M.; McGregor, T. L.; Lieske, J. C. Lumasiran, an RNAi Therapeutic for Primary Hyperoxaluria Type 1. *New England journal of medicine* **2021**, *384* (13), 1216−1226.

(8) Ray, K. K.; Wright, R. S.; Kallend, D.; Koenig, W.; Leiter, L. A.; Raal, F. J.; Bisch, J. A.; Richardson, T.; Jaros, M.; Wijngaard, P. L. J.; Kastelein, J. J. P. Two Phase 3 Trials of Inclisiran in Patients with Elevated LDL Cholesterol. *New England Journal of Medicine* **2020**, *382* (16), 1507−1519.

(9) Nair, J. K.; Willoughby, J. L.; Chan, A.; Charisse, K.; Alam, M. R.; Wang, Q.; Hoekstra, M.; Kandasamy, P.; Kel'in, A. V.; Milstein, S.; Taneja, N.; O'Shea, J.; Shaikh, S.; Zhang, L.; van der Sluis, R. J.; Jung, M. E.; Akinc, A.; Hutabarat, R.; Kuchimanchi, S.; Fitzgerald, K.; Zimmermann, T.; van Berkel, T. J.; Maier, M. A.; Rajeev, K. G.; Manoharan, M. Multivalent N-acetylgalactosamine-conjugated siRNA localizes in hepatocytes and elicits robust RNAi-mediated gene silencing. *J. Am. Chem. Soc.* **2014**, *136* (49), 16958−16961.

(10) Akinc, A.; Querbes, W.; De, S.; Qin, J.; Frank-Kamenetsky, M.; Jayaprakash, K. N.; Jayaraman, M.; Rajeev, K. G.; Cantley, W. L.; Dorkin, J. R.; Butler, J. S.; Qin, L.; Racie, T.; Sprague, A.; Fava, E.; Zeigerer, A.; Hope, M. J.; Zerial, M.; Sah, D. W.; Fitzgerald, K.; Tracy, M. A.; Manoharan, M.; Koteliansky, V.; Fougerolles, A.; Maier, M. A. Targeted delivery of RNAi therapeutics with endogenous and exogenous ligand-based mechanisms. *Mol. Ther* **2010**, *18* (7), 1357−1364.

(11) Ryals, R. C.; Patel, S.; Acosta, C.; McKinney, M.; Pennesi, M. E.; Sahay, G. The effects of PEGylation on LNP based mRNA delivery to the eye. *PLoS One* **2020**, *15* (10), No. e0241006.

(12) Sposito, A. C.; Zimetti, F.; Barreto, J.; Zanotti, I. Lipid trafficking in cardiovascular disease. *Adv. Clin Chem.* **2019**, *92*, 105−140.

(13) Chang, T. Y.; Chang, C. C.; Ohgami, N.; Yamauchi, Y. Cholesterol sensing, trafficking, and esterification. *Annu. Rev. Cell Dev Biol.* **2006**, *22*, 129−157.

(14) Sago, C. D.; Lokugamage, M. P.; Paunovska, K.; Vanover, D. A.; Monaco, C. M.; Shah, N. N.; Gamboa Castro, M.; Anderson, S. E.; Rudoltz, T. G.; Lando, G. N.; Munnilal Tiwari, P.; Kirschman, J. L.; Willett, N.; Jang, Y. C.; Santangelo, P. J.; Bryksin, A. V.; Dahlman, J. E. High-throughput in vivo screen of functional mRNA delivery identifies nanoparticles for endothelial cell gene editing. *Proc. Natl. Acad. Sci. U. S. A.* **2018**, *115* (42), E9944−E9952.

(15) Dahlman, J. E.; Barnes, C.; Khan, O.; Thiriot, A.; Jhunjunwala, S.; Shaw, T. E.; Xing, Y.; Sager, H. B.; Sahay, G.; Speciner, L.; Bader, A.; Bogorad, R. L.; Yin, H.; Racie, T.; Dong, Y.; Jiang, S.; Seedorf, D.; Dave, A.; Sandu, K. S.; Webber, M. J.; Novobrantseva, T.; Ruda, V. M.; Lytton-Jean, A. K. R.; Levins, C. G.; Kalish, B.; Mudge, D. K.; Perez, M.; Abezgauz, L.; Dutta, P.; Smith, L.; Charisse, K.; Kieran, M. W.; Fitzgerald, K.; Nahrendorf, M.; Danino, D.; Tuder, R. M.; von Andrian, U. H.; Akinc, A.; Schroeder, A.; Panigrahy, D.; Kotelianski, V.; Langer, R.; Anderson, D. G. In vivo endothelial siRNA delivery using polymeric nanoparticles with low molecular weight. *Nat. Nanotechnol* **2014**, *9* (8), 648−655.

(16) Lokugamage, M. P.; Sago, C. D.; Gan, Z.; Krupczak, B. R.; Dahlman, J. E. Constrained Nanoparticles Deliver siRNA and sgRNA to T Cells In Vivo without Targeting Ligands. *Adv. Mater.* **2019**, *31* (41), No. 1902251.

(17) Kauffman, K. J.; Oberli, M. A.; Dorkin, J. R.; Hurtado, J. E.; Kaczmarek, J. C.; Bhadani, S.; Wyckoff, J.; Langer, R.; Jaklenec, A.; Anderson, D. G. Rapid, Single-Cell Analysis and Discovery of Vectored mRNA Transfection In Vivo with a loxP-Flanked tdTomato Reporter Mouse. *Mol. Ther Nucleic Acids* **2018**, *10*, 55−63.

(18) Cheng, Q.; Wei, T.; Farbiak, L.; Johnson, L. T.; Dilliard, S. A.; Siegwart, D. J. Selective organ targeting (SORT) nanoparticles for tissue-specific mRNA delivery and CRISPR-Cas gene editing. *Nat. Nanotechnol* **2020**, *15* (4), 313−320.

(19) Dilliard, S. A.; Cheng, Q.; Siegwart, D. J. On the mechanism of tissue-specific mRNA delivery by selective organ targeting nanoparticles. *Proc. Natl. Acad. Sci. U. S. A.* **2021**, *118* (52), 2109256118.

(20) Patel, S.; Kim, J.; Herrera, M.; Mukherjee, A.; Kabanov, A. V.; Sahay, G. Brief update on endocytosis of nanomedicines. *Advanced drug delivery reviews* **2019**, *144*, 90−111.

(21) Gilleron, J.; Querbes, W.; Zeigerer, A.; Borodovsky, A.; Marsico, G.; Schubert, U.; Manygoats, K.; Seifert, S.; Andree, C.; Stoter, M.; Epstein-Barash, H.; Zhang, L.; Koteliansky, V.; Fitzgerald, K.; Fava, E.; Bickle, M.; Kalaidzidis, Y.; Akinc, A.; Maier, M.; Zerial, M. Image-based analysis of lipid nanoparticle-mediated siRNA delivery, intracellular trafficking and endosomal escape. *Nat. Biotechnol.* **2013**, *31* (7), 638−646.

(22) Paunovska, K.; Sago, C. D.; Monaco, C. M.; Hudson, W. H.; Castro, M. G.; Rudoltz, T. G.; Kalathoor, S.; Vanover, D. A.; Santangelo, P. J.; Ahmed, R.; Bryksin, A. V.; Dahlman, J. E. A Direct Comparison of in Vitro and in Vivo Nucleic Acid Delivery Mediated by Hundreds of Nanoparticles Reveals a Weak Correlation. *Nano Lett.* **2018**, *18* (3), 2148−2157.

(23) Wood, R. J.; Volek, J. S.; Liu, Y.; Shachter, N. S.; Contois, J. H.; Fernandez, M. L. Carbohydrate restriction alters lipoprotein

https://doi.org/10.1021/acs.nanolett.2c01133
Nano Lett. XXXX, XXX, XXX−XXX

metabolism by modifying VLDL, LDL, and HDL subfraction distribution and size in overweight men. *J. Nutr.* **2006**, *136* (2), 384−389.
(24) Uhlén, M.; Fagerberg, L.; Hallström, B. M.; Lindskog, C.; Oksvold, P.; Mardinoglu, A.; Sivertsson, Å.; Kampf, C.; Sjöstedt, E.; Asplund, A.; Olsson, I.; Edlund, K.; Lundberg, E.; Navani, S.; Szigyarto, C. A.; Odeberg, J.; Djureinovic, D.; Takanen, J. O.; Hober, S.; Alm, T.; Edqvist, P. H.; Berling, H.; Tegel, H.; Mulder, J.; Rockberg, J.; Nilsson, P.; Schwenk, J. M.; Hamsten, M.; von Feilitzen, K.; Forsberg, M.; Persson, L.; Johansson, F.; Zwahlen, M.; von Heijne, G.; Nielsen, J.; Pontén, F. Proteomics. Tissue-based map of the human proteome. *Science* **2015**, *347* (6220), 1260419.
(25) Eskelinen, E. L. Roles of LAMP-1 and LAMP-2 in lysosome biogenesis and autophagy. *Mol. Aspects Med.* **2006**, *27* (5−6), 495−502.
(26) Andrejewski, N.; Punnonen, E. L.; Guhde, G.; Tanaka, Y.; Lullmann-Rauch, R.; Hartmann, D.; von Figura, K.; Saftig, P. Normal lysosomal morphology and function in LAMP-1-deficient mice. *J. Biol. Chem.* **1999**, *274* (18), 12692−12701.
(27) Cook, N. R.; Row, P. E.; Davidson, H. W. Lysosome associated membrane protein 1 (Lamp1) traffics directly from the TGN to early endosomes. *Traffic* **2004**, *5* (9), 685−699.
(28) Luzio, J. P.; Pryor, P. R.; Bright, N. A. Lysosomes: fusion and function. *Nat. Rev. Mol. Cell Biol.* **2007**, *8* (8), 622−632.
(29) Carlsson, S. R.; Fukuda, M. The lysosomal membrane glycoprotein lamp-1 is transported to lysosomes by two alternative pathways. *Arch. Biochem. Biophys.* **1992**, *296* (2), 630−639.
(30) Hu, B.; Zhong, L.; Weng, Y.; Peng, L.; Huang, Y.; Zhao, Y.; Liang, X. J. Therapeutic siRNA: state of the art. *Signal Transduct Target Ther* **2020**, *5* (1), 101.
(31) Chen, D.; Love, K. T.; Chen, Y.; Eltoukhy, A. A.; Kastrup, C.; Sahay, G.; Jeon, A.; Dong, Y.; Whitehead, K. A.; Anderson, D. G. Rapid discovery of potent siRNA-containing lipid nanoparticles enabled by controlled microfluidic formulation. *J. Am. Chem. Soc.* **2012**, *134* (16), 6948−6951.
(32) Sago, C. D.; Lokugamage, M. P.; Islam, F. Z.; Krupczak, B. R.; Sato, M.; Dahlman, J. E. Nanoparticles That Deliver RNA to Bone Marrow Identified by in Vivo Directed Evolution. *J. Am. Chem. Soc.* **2018**, *140* (49), 17095−17105.
(33) Baden, L. R.; El Sahly, H. M.; Essink, B.; Kotloff, K.; Frey, S.; Novak, R.; Diemert, D.; Spector, S. A.; Rouphael, N.; Creech, C. B.; McGettigan, J.; Khetan, S.; Segall, N.; Solis, J.; Brosz, A.; Fierro, C.; Schwartz, H.; Neuzil, K.; Corey, L.; Gilbert, P.; Janes, H.; Follmann, D.; Marovich, M.; Mascola, J.; Polakowski, L.; Ledgerwood, J.; Graham, B. S.; Bennett, H.; Pajon, R.; Knightly, C.; Leav, B.; Deng, W.; Zhou, H.; Han, S.; Ivarsson, M.; Miller, J.; Zaks, T.; Group, C. S. Efficacy and Safety of the mRNA-1273 SARS-CoV-2 Vaccine. *N Engl J. Med.* **2021**, *384* (5), 403−416.
(34) Polack, F. P.; Thomas, S. J.; Kitchin, N.; Absalon, J.; Gurtman, A.; Lockhart, S.; Perez, J. L.; Pérez Marc, G.; Moreira, E. D.; Zerbini, C.; Bailey, R.; Swanson, K. A.; Roychoudhury, S.; Koury, K.; Li, P.; Kalina, W. V.; Cooper, D.; Frenck, R. W.; Hammitt, L. L.; Türeci, Ö.; Nell, H.; Schaefer, A.; Ünal, S.; Tresnan, D. B.; Mather, S.; Dormitzer, P. R.; Şahin, U.; Jansen, K. U.; Gruber, W. C. Safety and Efficacy of the BNT162b2 mRNA Covid-19 Vaccine. *New England Journal of Medicine* **2020**, *383* (27), 2603−2615.
(35) Mui, B. L.; Tam, Y. K.; Jayaraman, M.; Ansell, S. M.; Du, X.; Tam, Y. Y.; Lin, P. J.; Chen, S.; Narayanannair, J. K.; Rajeev, K. G.; Manoharan, M.; Akinc, A.; Maier, M. A.; Cullis, P.; Madden, T. D.; Hope, M. J. Influence of Polyethylene Glycol Lipid Desorption Rates on Pharmacokinetics and Pharmacodynamics of siRNA Lipid Nanoparticles. *Mol. Ther Nucleic Acids* **2013**, *2*, No. e139.
(36) Paunovska, K.; Loughrey, D.; Sago, C. D.; Langer, R.; Dahlman, J. E. Using Large Datasets to Understand Nanotechnology. *Adv. Mater.* **2019**, *31* (43), No. 1902798.
(37) Paunovska, K.; Gil, C. J.; Lokugamage, M. P.; Sago, C. D.; Sato, M.; Lando, G. N.; Gamboa Castro, M.; Bryksin, A. V.; Dahlman, J. E. Analyzing 2000 in Vivo Drug Delivery Data Points Reveals Cholesterol Structure Impacts Nanoparticle Delivery. *ACS Nano* **2018**, *12* (8), 8341−8349.
(38) Solberg, L. B.; Stang, E.; Brorson, S. H.; Andersson, G.; Reinholt, F. P. Tartrate-resistant acid phosphatase (TRAP) co-localizes with receptor activator of NF-KB ligand (RANKL) and osteoprotegerin (OPG) in lysosomal-associated membrane protein 1 (LAMP1)-positive vesicles in rat osteoblasts and osteocytes. *Histochem Cell Biol.* **2015**, *143* (2), 195−207.
(39) Yamashima, T.; Tonchev, A. B.; Tsukada, T.; Saido, T. C.; Imajoh-Ohmi, S.; Momoi, T.; Kominami, E. Sustained calpain activation associated with lysosomal rupture executes necrosis of the postischemic CA1 neurons in primates. *Hippocampus* **2003**, *13* (7), 791−800.
(40) Hatit, M. Z. C.; Lokugamage, M. P.; Dobrowolski, C. N.; Paunovska, K.; Ni, H.; Zhao, K.; Vanover, D.; Beyersdorf, J.; Peck, H. E.; Loughrey, D.; Sato, M.; Cristian, A.; Santangelo, P. J.; Dahlman, J. E. Species-dependent in vivo mRNA delivery and cellular responses to nanoparticles. *Nat. Nanotechnol.* **2022**, *17*, 310−318.
(41) Lokugamage, M. P.; Vanover, D.; Beyersdorf, J.; Hatit, M. Z. C.; Rotolo, L.; Echeverri, E. S.; Peck, H. E.; Ni, H.; Yoon, J.-K.; Kim, Y.; Santangelo, P. J.; Dahlman, J. E. Optimization of lipid nanoparticles for the delivery of nebulized therapeutic mRNA to the lungs. *Nat. Biomed.* **2021**, *5*, 1059−1068.

https://doi.org/10.1021/acs.nanolett.2c01133
Nano Lett. XXXX, XXX, XXX−XXX